

# Adsorption Isotherms and Kinetics Studies of a Cationic and Anionic Dye Removal from Aqueous Solution Onto *Raphia Farinifera* Biomass

Loretta Chukwudumebi Overah

Chemistry Department, Faculty of Science, Delta State University, Abraka, Delta State.

\*Corresponding author. E-mail:overahrubya@yahoo.com. Tel.+2348166185591

Accepted 31st May 2021

The adsorption of methylene blue (MB) a cationic dye and methyl orange (MO) an anionic dye from aqueous solution onto *Raphia farinifera* as an inexpensive and renewable biosorbent, was investigated in this study through batch experiments in order to determine the effect of pH, contact time and initial dyes concentration at a temperature of 27°C. The process proved to be pH-dependent reaching optimum at pH 12 and 4 for methylene blue and methyl orange dyes respectively within 90 min. Also, the adsorption percentage decreased with increased dye concentration. Five adsorption isotherm models namely: Langmuir, Freundlich, Dubinin Radush-kevich, Temkin and Scatchard isotherm models were applied to analyze the relationship between the amount of dye adsorbed and the remaining in solution. From the result, both Langmuir and Freundlich isotherm models suitably described the mechanism of the sorption process, but the Freundlich isotherm provided a better fit, indicating multi-layer adsorption onto heterogeneous binding sites. The non-linear conformity of the Scatchard isotherm plot to the equilibrium adsorption data further supported this fact. Kinetic analysis showed that both dyes followed the pseudo second-order and Elovich kinetic mechanisms. However, MO adsorption kinetics also aligned with the intra-particle diffusion model to a reasonable extent. All these findings suggest that *Raphia farinifera* is useable as an effective material for separation of MB and MO dyes from aqueous systems.

**Key words:** Adsorption, Freundlich isotherm, methylene blue, methyl orange, Pseudosecond-order, *Raphia farinifera*, Scatchard isotherm.

## INTRODUCTION

The release of dyes into water bodies is a major hazard facing the inhabitant plants, animals and humans because of their toxicity, carcinogenic and mutagenic effects. It is alarming for aesthetic and toxicological reasons (Metivier-Pignon et al., 2003). Printing houses, paper-making industries, textile industries and dye houses make use of synthetic dyes, of which a substantial amount makes its way into the effluents and end up in surface and ground water through the discharge of these effluents in water bodies. This constitutes a major source of pollution of the aquatic environment (Aksu, 2005; Attia et al., 2008). Almost 15% of dyestuffs used in the industries concerned are lost to effluents during the industrial operations

such as manufacturing, processing and packaging (Gupta et al., 2012). Methylene blue, a thiamine and cationic dye, is extensively employed in fabric and paper dyeing, food coloring, and temporary hair coloring dyes. Exposure to methylene blue (MB) causes short periods of difficulty in breathing and eye burns which results in permanent eye injuries, while oral consumption causes a sensational burning effect and instigates profuse sweating, nausea and vomiting, confusion or mental imbalance and methaemoglobinemia (Ghosh and Bhattacharyya, 2002).

Methyl orange (sodium-(4(dimethylamino)phenyl) diazenylbenzene-1-sulfonate) is a pH indicator commonly used in titration because of its ability to exhibit distinct

and clear color variance at different pH values. The production and utilization of methyl orange as a textile dye and pH indicator results to its eventual discharge into the environment through different waste streams. Therefore, treating the dye-containing effluent is paramount due to their harmful impact on the receiving water bodies and ultimately on the aquatic and terrestrial animals including man.

Dye-loaded industrial effluent treatment poses a great challenge amongst wastewaters treatment procedures not just because of their toxicity, high biological and chemical oxygen demands and total suspended solids but mainly for their color, which makes their presence visually obvious and easily identified (Aksu, 2005). Thus, dye-containing wastewaters must be treated to conserve the aesthetic value and safety of the environment and to protect human health. However, because these dyes are mainly synthetic with complex aromatic structure which makes them stable and resistant to biodegradation and photo degradation, their treatment in industrial wastewaters is difficult (Gupta, 2009; Lorenc-Grabowska and Gryglewicz, 2007). Nevertheless, the removal of dyes from aqueous solution or effluents through the process of adsorption has been proven to overcome this difficulty to a reasonable extent due to its simplicity, efficiency and inexpensiveness (Kyzas et al., 2012). The adsorption process entails the accumulation of a contaminant in water on a solid surface or interface between two phases. The component being attached by a physical or chemical bond is then separated out of the liquid phase (Demirbas et al., 2008). The success of an adsorption process largely depends on the use of an ideal adsorbent. What makes an adsorbent ideal is not only a good adsorption potential but also its availability in abundance among other factors (Han et al., 2008).

In the last decade, many low-cost, non-conventional adsorbents such as orange peelings, rice hull ash, mango seed kernel powder, sawdust, eucalyptus bark, pine needle, prawn shell activated carbon, sugarcane bagasse and more, have been evaluated and found beneficial for heavy metal and dye removal from aqueous medium in the process

known as biosorption (Adsorption using materials of biological origin) (Sud et al., 2008). This technique aims at the removal and recovery of dyes, metals and particulate matter from solution by the use of low-cost biological materials which may be dead or living microorganisms, plant materials, seaweeds and agro-wastes (Mustapha and Halimoon, 2015). The present study is aimed at testing the usability of *Raphia farinifera* for the abstraction of MB and MO dyes from an aqueous medium, while relating its potential with some of its surface characteristics such as its point of zero charge, surface area, surface acidic and basic oxygen groups and the chemical make-up of its active sites. The readiness of the fruit fibres of *Raphia farinifera* to adsorb dyes makes it ideal for use in fancy items and prompts the idea of testing the fruit pericarp (the golden-brown scales) for dye adsorption. Also, it is inexpensive and abundant mainly in the swampy regions of Nigeria. To further keep the cost of the adsorption process at a minimum, the Rf was used in this study without any chemical treatment. The influence of solution pH, contact time and initial MB and MO dyes concentrations were investigated. Furthermore, the kinetics and equilibrium adsorption isotherm of the process were evaluated using known models for each study namely; the Pseudo-first-order, pseudo-second-order, intra-particle diffusion and Elovich models for kinetics study while the Freundlich, Langmuir, Dubinin-Radushkevich, Temkin and Scatchard models were applied for isotherm study. As far as literature is concerned, no study has been done evaluating *Raphia farinifera* for MB and MO dyes adsorption. The fruits are shown in Figure 1A.

## MATERIALS AND METHODS

### Collection, Preparation and characterization of Biomass

The ripe fruit bunch of *Raphia farinifera* was collected from swamps in Sapele, Delta State, Nigeria. It was then prepared and characterized to determine its point of Zero charge (pHpzc), following the method described in our previous work (Overah et al., 2019).

### Preparation of stock solutions

Methylene blue and methyl orange dyes used were of analytical grade. 1000 mg each of MB

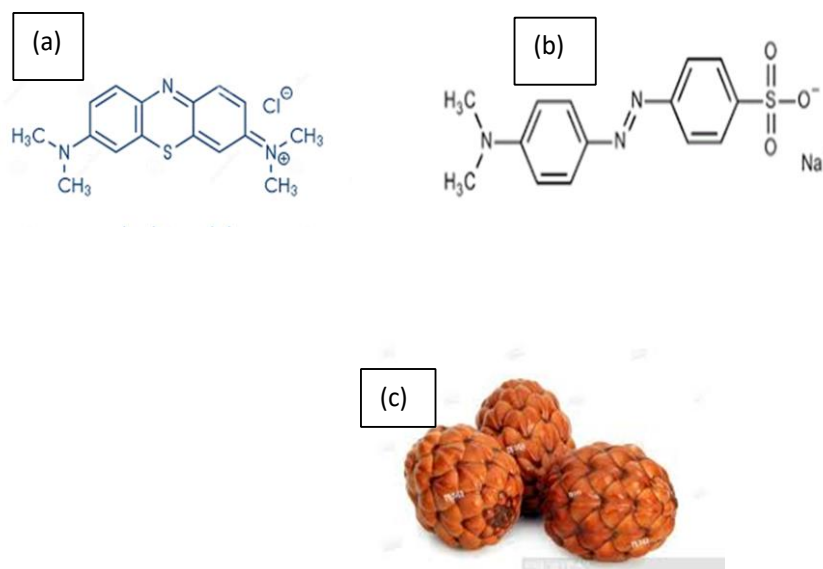


**Figure 1A.** (a) methylene blue (b) methyl orange (c) *Raphia farinifera* fruit.

and MO dyes were weighed and dissolved into 1000 ml of deionized water to produce 1000 mg/L stock solution of each dye. These solutions were then stored in large glass vials and stored away from light.

#### The dilution of stock solutions

The serial dilutions of both dyes were prepared from each of the stock solutions in a *series* of repeated dilution steps. The concentrations which were obtained from the serial dilution are; 62.5, 31.2, 15.625, 7.8125 and 3.9 mg/ml. The calibration curves of MB and MO at 667 nm and 505 nm respectively, were obtained using a UV spectrometer, as straight-line plots of the concentrations versus the corresponding absorbance.

#### Adsorption studies

The effects of pH, contact time and initial dye concentration on the removal process were investigated in a batch mode. To study the effect of pH, the dye solutions were adjusted to the various pH values from 2 to 14, either by adding a very minute amount of concentrated or dilute hydrochloric acid or concentrated or dilute sodium hydroxide as the case required. Thereafter, a 25 ml aliquot of each dye solution of a concentration of 62.5 mg/L was agitated with 0.1 g of the adsorbent for 2 h at 27°C and centrifuged at 2000 rpm. The supernatant was then analyzed for concentration left using

UVspectrophotometer.

In studying the effect of contact time, 0.1g of the Rf was contacted with 25 ml of the 50 mg/L dye solutions at varied time intervals of 10, 20, 30, 40, 50, 60, 70, 80, 90, and 100 min respectively, at the optimum pH obtained per dye and at 27°C. Afterwards, the suspension was centrifuged and the residual dye concentration of the supernatant was measured by UV spectroscopy.

The effect of initial dye concentration was investigated by agitating 25 ml of the dye solutions of five different concentrations (62.5, 31.2, 15.6, 7.8, and 3.9 mg/L) with 0.1 g of Rf in 100 ml conical flasks at the optimum time and pH determined for each dye adsorption at 27°C and a speed of 150 rpm.

#### Estimation of dye content

The residual concentrations of MB and MO dyes in this study were determined using the ultraviolet spectrophotometer (UV) at wavelengths of 667 nm and 505 nm respectively. The calibration curves of methylene blue and methyl orange at their respective wavelengths were obtained as straight-line plots of concentrations (which were prepared through serial dilutions) and corresponding absorbance. The equation of each linear graph, generated by OriginPro 6.0 and displayed on the graph was used to calculate the subsequent residual concentrations of the dyes after contact with the *Raphia*

*farinifera* biomass. That is:

$$y = mx \dots\dots\dots(1)$$

where m and y are the variables and x represents the slope and is analogous to the Beer-Lambert equation:

$$A = ECl \dots\dots\dots(2)$$

where l is cell path length taken as unity, y is equivalent to the absorbance, A; m is the slope equivalent to the molar absorptivity, E; and x is equivalent to the concentration, C. However, in this case, the equation of the calibration curve has an intercept. Therefore, the subsequent concentrations were simply calculated by inserting the measured absorbance into the equation of the calibration curve as y and solving for the corresponding concentration, x.

**Statistical analysis**

All data obtained in this study were analyzed by making appropriate plots using the originPro 6.1 software, while the kinetic and equilibrium isotherm data analyses were done as described in the sub sections below.

**Data analysis**

The efficiency of the adsorption process is reported as a percentage using the equation:

$$\% \text{ Dye Removal} = \frac{C_0 - C_e}{C_0} \times 100 \dots\dots\dots(3)$$

The amount of methylene blue in milligrams removed per gram of the biosorbent during the experiment was determined using the expression:

$$q_e = \frac{V}{m} (C_0 - C_e) \dots\dots\dots(4)$$

Where  $c_e$  = final dye concentration at equilibrium (mg/L),  $c_o$ = initial dye concentration (mg/L),  $V$ = volume of dye solution (L),  $m$ = mass or dose of the biomass (g) and  $q_e$  = amount of dye adsorbed per gram of the biomass (mg g<sup>-1</sup>).

**Adsorption Isotherms**

The  $q_e$  and  $C_e$  data gotten from the study of the initial dye concentration were tested on five

adsorption isotherm models namely: the Langmuir, Freundlich, Scatchard, Dubinin-Radushkevich and Temkin isotherms. The Langmuir equation suggests monolayer coverage on a surface which contains a finite number of homogenous or identical active sites. The linear form of the equation is (Perez et al., 2007):

$$\frac{C_e}{q_e} = \frac{1}{K_L q_m} + \frac{C_e}{q_m} \dots\dots\dots(5)$$

$q_m$  represents the Langmuir maximum monolayer adsorption capacity (mg/g);  $K_L$ , the Langmuir constant. A graph of  $C_e/q_e$  vs  $C_e$  was plotted from which  $q_m$  and  $K_L$  were estimated from the slope and intercept respectively.

The Freundlich equation accounts for an adsorbate's adsorption onto a heterogeneous surface having non-identical active sites and given linearly as (Freundlich, 1906; Overah, 2011):

$$\text{Log } q_e = \text{log } K_f + \frac{1}{n} \text{log } C_e \dots\dots\dots(6)$$

Where,  $K_f$  stands for the Freundlich constant and  $n$  is the adsorption intensity. A plot of  $\text{log } q_e$  vs  $\text{log } C_e$ , gives a straight line in which  $1/n$  is the slope and

$\text{log } K_f$  is the intercept.

The Scatchard equation is given as (Anirudhan and Suchithra, 2010; Akpomie et al., 2015):

$$q_e / C_e = q_m b - q_e b \dots\dots\dots(7)$$

Where  $q_m$  (mg/g) and  $b$  (L/mg) are the Scatchard isotherm parameters. Information about the adsorbate-adsorbent interactions can be deduced from the shape of the plot. When the plot of  $q_e/C_e$  against  $q_e$ , is a straight line, then the binding sites on the adsorbent are homogeneous or uniform or having the same type of binding site, but a non-linear outcome implies that the binding sites on the biosorbent's surface are heterogeneous (Anirudhan and Suchithra, 2010; Akpomie et al., 2015).

The Dubinin-Radushkevich (D-R) isotherm is an empirical model where the adsorption mechanism follows a pore-filling pattern and not a layer-by-layer surface coverage. It focuses on the energy of the adsorption process as well as the porosity of the biomass. The value of this energy

of adsorption is a determinant as to whether the adsorbate-adsorbent interaction is physical or chemical (Dubinin 1960, Horsfall et al., 2004). It is mathematically expressed as:

$$\ln q_e = \ln q_o - \beta \epsilon^2 \dots\dots\dots(8)$$

Where  $q_e$  is as earlier defined,  $q_o$  is the maximum adsorption capacity,  $\beta$  is the activity coefficient from which the mean energy sorption,  $E(\text{kJ/mol})$  may be estimated from equation (5) and  $\epsilon$  is the Polanyi potential. The parameters,  $E$  and  $\epsilon$  are expressed as;

$$\text{and } E = \sqrt{1/2\beta} \dots\dots\dots(9)$$

$$\epsilon = RT \ln (1 + 1/C_e) \dots\dots\dots(10)$$

Where  $T$  and  $R$  are the temperature in Kelvin and gas constant ( $\text{J mol}^{-1}\text{K}^{-1}$ ), respectively. The values of  $q_o$  ( $\text{mg/g}$ ) and  $\beta$  ( $\text{mol}^2/\text{kJ}^2$ ) can be calculated from the intercept and slope of the graph of  $\ln q_e$  vs  $\epsilon^2$  respectively.

The Temkin isotherm postulates that the distribution of binding energy up to a certain maximum is uniform and also assumes a linear decline of the energy of adsorption while ignoring extreme conditions of very low and very high adsorbate concentrations. Temkin isotherm is mathematically stated as: (Inyibor et al., 2016; Yu et al., 2001):

$$q_e = B \ln A + B \ln C_e \dots\dots\dots(11)$$

"A" ( $\text{L/g}$ ) is the Temkin isotherm constant while  $B$  is a constant related to the energy of adsorption, expressed as:

$B = RT/b$  where  $b$  ( $\text{J mol}^{-1}$ ) is the Temkin constant associated with the heat of adsorption,  $T$  ( $\text{K}$ ) is the absolute temperature and  $R$  is the gas constant ( $8.314 \text{ J mol}^{-1}\text{K}^{-1}$ ). The constants,  $A$  and  $B$  may be calculated from the intercepts and slope respectively of the plot of  $q_e$  vs  $\ln C_e$ .

**Kinetics of the adsorption**

It is not enough for an adsorbent to have good adsorption capacity but the rate of adsorption is also important in defining the adsorbent efficiency. The study of the adsorption

kinetics is very important in determining the adsorbent's efficiency because it describes the uptake rate which determines the resident time of adsorbate ions at the solid-liquid boundary. Also, the adsorption rate constant can be used to compare the performance of various adsorbents (Demirbas et al., 2008). Various kinetic models have been adopted to describe the mechanism of batch adsorption processes namely: pseudo-first-order, pseudo-second-order, intra-particle diffusion and Elovich kinetic models. In this study, the adsorption kinetics data were fitted to these four kinetics models to see which model best fits the data.

**The pseudo-first-order**

The pseudo-first-order rate is generally expressed linearly as:

$$\log(q_e - q_t) = \log q_e - \frac{k_1}{2.303} t \dots\dots\dots(12)$$

Where  $q_t$  and  $q_e$  are the amount of adsorbate adsorbed in milligrams per gram of adsorbent at time,  $t$  and at equilibrium respectively and  $k_1$  ( $\text{min}^{-1}$ ) is the pseudo-first-order rate constant. A plot of  $\log(q_e - q_t)$  against  $t$  should be linear (if this mechanism applies to the process) from which  $q_e$  and  $k_1$  are calculated from the graph's intercept and slope respectively (Overah, 2011).

**The pseudo-second-order**

The pseudo-second-order kinetics model can be expressed by the linear form (Ho and McKay, 1998):

$$\frac{t}{q_e} = \left(\frac{1}{k_2 q_e^2}\right) + \left(\frac{t}{q_e}\right) \dots\dots\dots(13)$$

Where  $k_2$  ( $\text{g mg}^{-1} \text{ min}^{-1}$ ) is the Pseudo-second-order rate constant. By plotting  $t/q_t$  against  $t$ , the values of  $k_2$  and  $q_e$  are determined from the graph's intercept and slope, respectively (Hamza et al., 2013; Overah, 2011).

**Intra-particle diffusion**

In some cases, the mechanism of diffusion of solute through adsorbent solid may not be described by either the pseudo-first-order or pseudo-second-order kinetics models. In such cases, the kinetics data may be analyzed by the intra-particle diffusion model which is described by Weber and Morris (1963) and is expressed

by the Equation (Demirbas et al., 2008):

$$q_t = k_{id}(t)^{0.5} + C \dots\dots\dots (14)$$

where  $q_t$  is as already defined,  $C$  ( $\text{mg g}^{-1}$ ) is the adsorption constant and  $k_{id}$  ( $\text{mg g}^{-1} \text{min}^{-1/2}$ ) is the intra-particle diffusion rate constant. When intra-particle diffusion is the rate-limiting step of the adsorption process,  $q_t$  varies linearly with  $t^{0.5}$ .

### Elovich

This model was initially used to investigate the sorption of gas on a solid surface, but is also applicable in describing the kinetics in aqueous phase adsorption (Hamza et al., 2013). It is mathematically expressed as:

$$q_t = \frac{1}{\beta} \ln(\alpha\beta) + \frac{1}{\beta} \ln t \dots\dots\dots (15)$$

where  $\alpha$  ( $\text{mg g}^{-1} \text{min}^{-1}$ ) and  $\beta$  ( $\text{g mg}^{-1}$ ) are the initial adsorption rate and desorption constant, respectively. A linear plot of  $q_t$  against  $\ln(t)$  depicts the suitability of the model, with the slope and intercept as  $(1/\beta)$  and  $(1/\beta)\ln(\alpha\beta)$  respectively.

## RESULTS AND DISCUSSION

### Review of the characteristics of the Rf

The result of the experiment to determine the pH<sub>pzc</sub> of the Rf reported by Overah et al. (2019), shows that the Rf surface has a surface charge of 6.5. This is the pH at which the biosorbent's surface is electrically neutral. This

means that both the negative charges and the positive charges are equal at this pH. The implication of this is that below this pH, there will be a net positive charge which should enhance the electrostatic attraction of anionic species to the adsorbent while above the pH<sub>pzc</sub>, the surface of the biomass has a net negative charge which should favour the electrostatic attraction of cationic species (Lazarevic et al., 2007). Also, FTIR investigation of the Rf carried out in our earlier work, showed that carboxylic C=O and C-O groups were present as the main active sites with a total surface acidic oxygen groups of  $2.014 \text{ mMg}^{-1}$  determined by the Boehm titration. Surface basic oxygen groups were reported to be completely absent in the study. The BET surface area of Rf was also reported as  $0.939 \text{ m}^2\text{g}^{-1}$  (Overah et al., 2019).

### UV measurements and estimation of concentrations

The calibration curves of methylene blue and methyl orange at 667 nm and 505 nm are the linear plots of the various concentrations which were prepared through serial dilutions versus the corresponding absorbance as shown in Table 1. The calibration curves are shown to have  $R^2$  values of 0.997 and 0.9998 for methylene blue and methyl orange, respectively (Figure 1B). The equation of each graph displayed on the graphs was used to calculate the residual concentrations of the dyes after contact with the *Raphia farinifera* biomass and measurement of the absorbance as explained in the methods section.

**Table 1.** Concentration and corresponding absorbance of methylene blue and methyl orange dyes.

Concentration (mg/L)	Absorbance Methylene blue @ 667 nm	Absorbance Methyl orange @ 505 nm
62.50	2.282	1.77
31.25	1.244	0.860
15.63	0.596	0.410
7.813	0.315	0.180
3.906	0.116	0.040

### Adsorption studies

#### Effect of pH

The result of the effect of pH on MB and MO uptake onto *Raphia farinifera* at  $27^\circ\text{C}$  and agitation speed of 120 rpm in 2 h is shown in Figure 2. It is shown in the figure that MB, a

cationic dye was adsorbed more at a high or alkaline pH. This is explained by the fact that at alkaline pH the biomass surface has a net negative charge which favors cationic adsorption, hence increased adsorption of MB is observed at higher pH. The optimum pH for MB adsorption

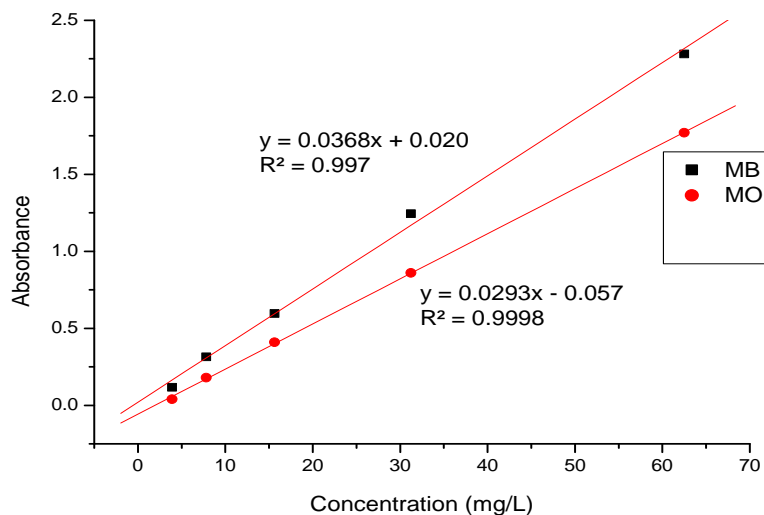


**Figure 1B.** Plot of absorbance against concentration for methylene blue and methyl orange dyes at 667 nm and 505 nm respectively.

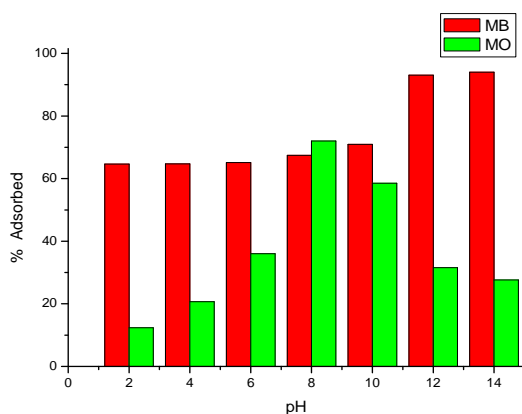


**Figure 2.** The effect of pH on the adsorption of MB and MO dyes onto *Raphia farinifera* at contact time 90 min, concentration 50 mg/L biomass 0.1g at a temperature of 27°C.

was therefore taken as pH 12, since a further increase to pH 14 had no significant effect on the amount adsorbed. Also, the pH<sub>pzc</sub> of the biomass surface is 6.5 and it is only expected that a cationic dye like MB will be adsorbed favourably at a pH above this. Khodaie et al. (2013) reported a similar result for the effect of pH on MB adsorption onto zinc chloride-activated corn husk carbon. On the other hand, methyl orange adsorption took a different course with varied pH values. There was a gradual increase in the amount adsorbed when pH was increased from 2 to 8 reaching a peak at pH 8. This unexpected outcome may be suggestive of the possibility of an overriding adsorption mechanism like complexation,

besides electrostatic attraction between unlike charges, since anionic dyes should be more adsorbed at low or acidic pH or in this case at a pH less than the pH<sub>zc</sub> of the adsorbent. A further increase in the pH value led to a decrease in the dye uptake probably due to repulsion between like (negative) charges. Therefore, the optimum pH for MO adsorption was taken as 8.

#### *Effect of time*

The result of this study (Figure 3) shows that the uptake of methylene blue was rapid at the start of the process with over 77% methylene blue adsorption achieved within 40 min and then continued to increase gradually until reaching equilibrium at 90 min with a removal efficiency of about 83%. Such behavior is typical where there are several adsorption sites on the biomass surface which gradually gets saturated with the dye at increasing contact times. The same trend is observed for MO adsorption. It was rapid initially but gradually, reached an optimum at 100 min. MB adsorption by Rf was not only more but also faster to reach equilibrium than MO adsorption. This could be as a result of the fact that MB, a heterocyclic aromatic compound is lighter in molecular weight (319.85 g) than MO (327.3 g) and can therefore travel faster in solution. Additionally, at optimum pH values determined for each dye, MB was adsorbed more than MO likely because the former is a cationic dye which would be more attracted to the anionic functional

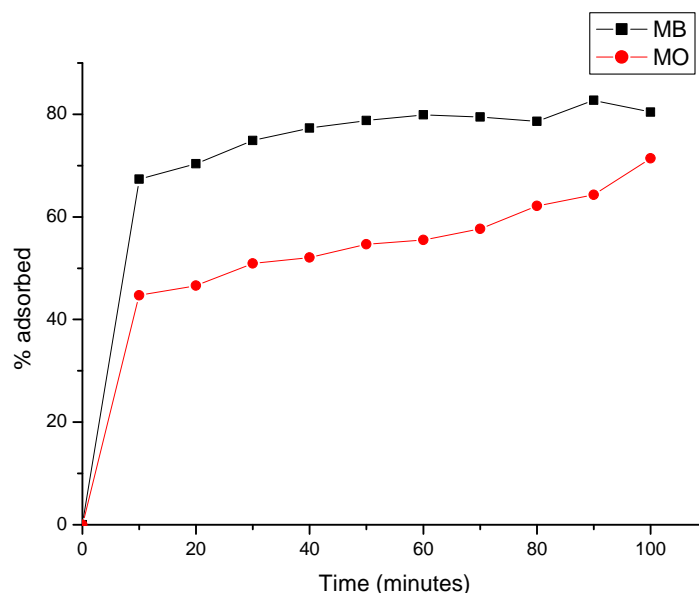


**Figure 3.** The effect of contact time on % adsorption of MB and MO onto *Raphia farinifera* at optimum pH, concentration 50 mg/L, biomass dose 0.1g at a temperature of 27°C.

groups determined on the Rf surface by FTIR studies. According to Salleh, (2011), for the same biosorbent, a cationic dye is usually better adsorbed than an anionic dye because the carboxyl group is a major functional group in agricultural adsorbents and is negatively charged. This enhances cationic dye uptake but inhibits the uptake of anionic dyes. To further support this, the Boehm titration to quantify the surface acidic and basic oxygen groups in our earlier work shows that only surface acidic groups like the carboxylic groups were present

on the Rf (Overah et al., 2019).

#### ***Effect of initial dye concentration***

The experimental result shows that the percentage removal of MB and MO dyes decreased with increase in the dyes concentration from 3.91 to 62.50 mg/l as shown in Figure 4. This may be due to the fact that at a lower concentration of the dye, less of it was available for adsorption compared with the amount of the active sites on the biomass.

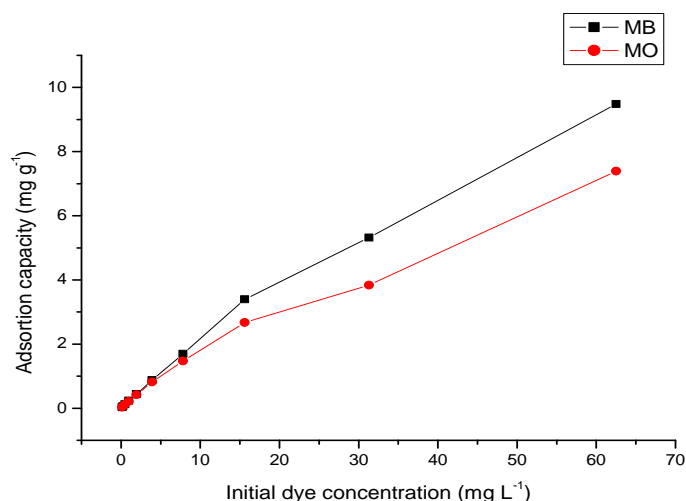


**Figure 4.** The effect of concentration on the percentage adsorption of MB and MO dyes onto *Raphia farinifera*. at optimum pH, contact time 90 min, biomass 0.1g at a temperature of 27°C.



That is, the biomass concentration was much more than the dye concentration. At higher concentration, more of the dye was available and high initial adsorbate concentration acts as a vital force to overcome the dye molecules' resistance to mass or bulk transfer from the aqueous phase to the solid-liquid interface.

### Adsorption isotherms

The results of the adsorption isotherm

modeling of the initial concentration data for MB and MO adsorption onto *Raphia farinifera* are presented in Figures 5-9. For the Langmuir isotherm model, the  $R^2$  values of 0.94918 and 0.92225 for MB and MO respectively (Figures 5), suggests that the Langmuir isotherm provides a good fit for the adsorption of both dyes onto *Raphia farinifera*. This implies that the adsorption of the dyes onto the *Raphia farinifera* biomass is monolayer in nature.

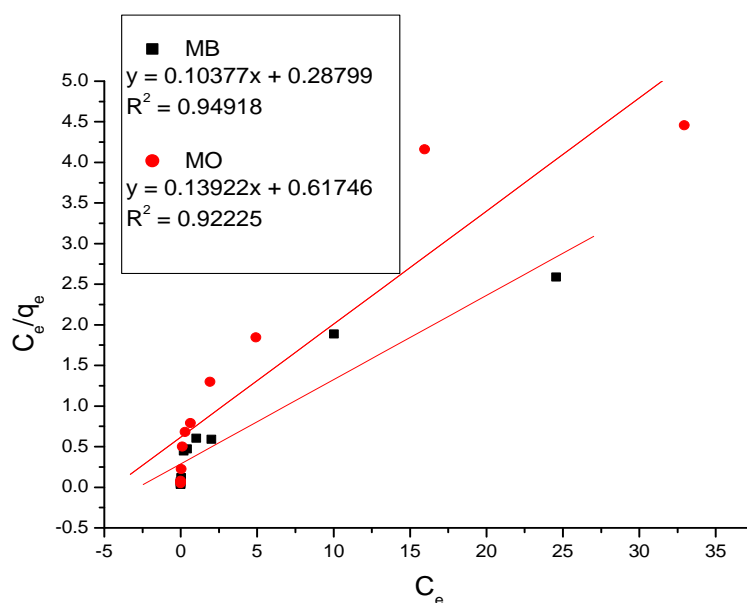


**Figure 5.** The Langmuir Isotherm for methylene blue and methyl orange dyes uptake onto *Raphia farinifera* at optimum pH, contact time 90 min, biomass 0.1g at a temperature of 27°C .

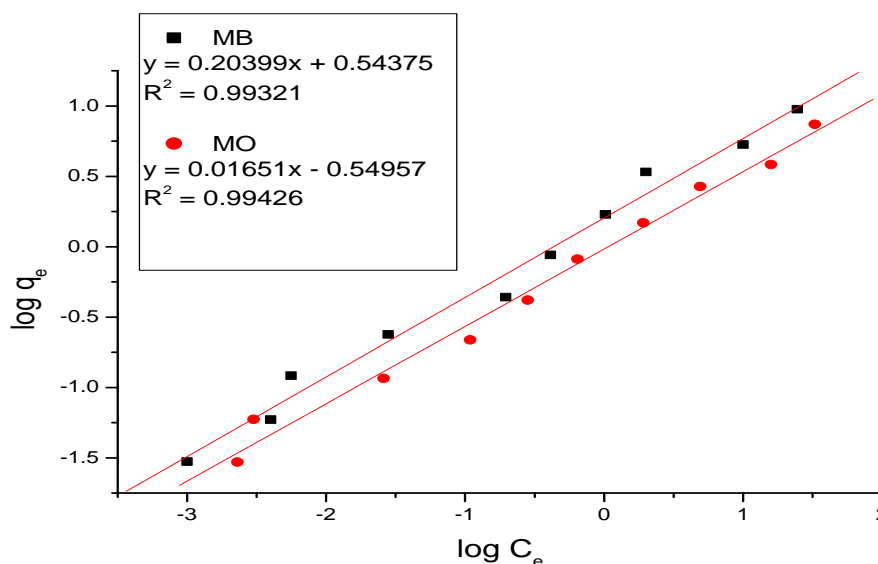


**Figure 6.** The Freundlich Isotherm plot for methylene blue and methyl orange dyes uptake onto *Raphia farinifera* at optimum pH, contact time 90 min, biomass 0.1g at a temperature of 27°C.

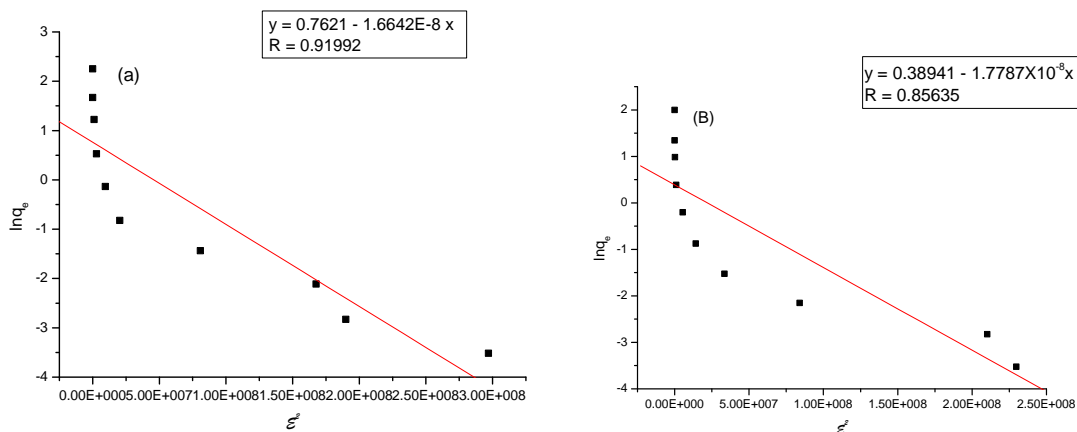


**Figure 7.** The Dubinin Radush-kevich Isotherm plot for (a) methylene blue (b) methyl orange dyes uptake onto *Raphia farinifera*. at optimum pH, contact time 90 min, biomass 0.1g at a temperature of 27°C.

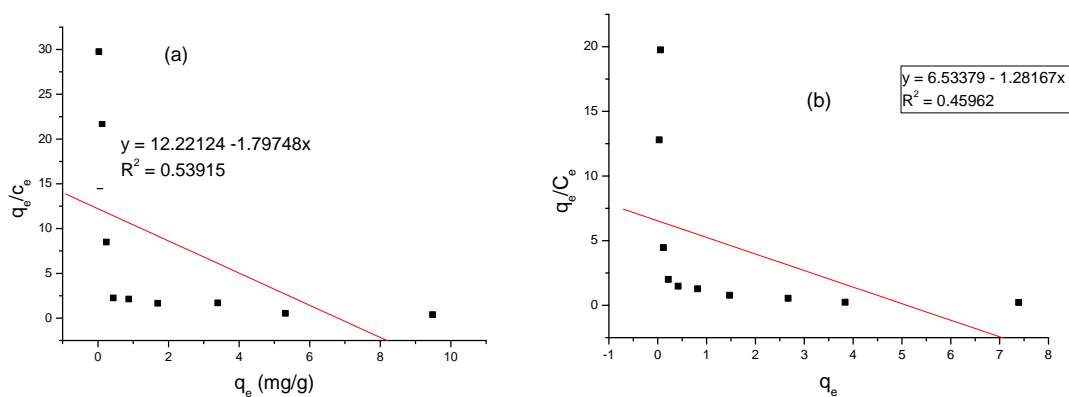


**Figure 8.** Scatchard plot for (a) MB and (b) MO at optimum conditions at optimum pH, contact time 90 min, biomass 0.1g at a temperature of 27°C.

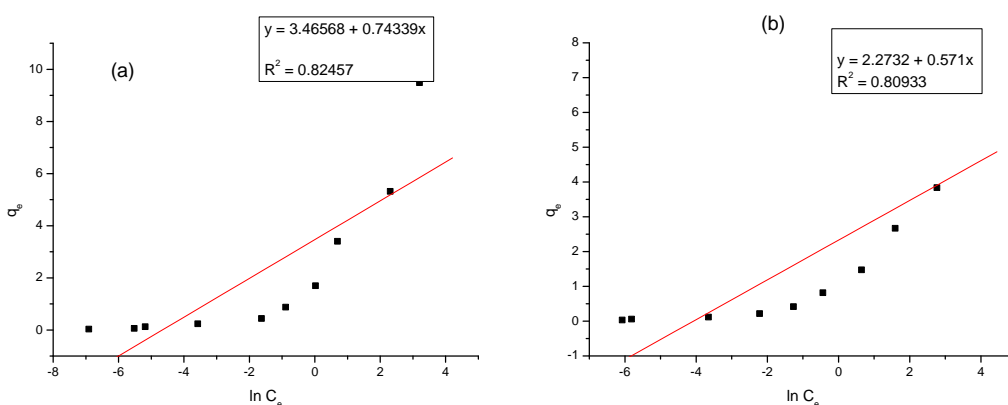


**Figure 9.** Temkin isotherm for (a) MB and (b) MO dyes uptake onto *Raphia farinifera* at optimum pH, contact time 90 min, biomass 0.1g at a temperature of 27°C.

The Langmuir monolayer adsorption capacity,  $q_m$  and the Langmuir constant,  $K_L$  were estimated from the slope and intercept respectively and presented in Table 2 with

other parameters. The Freundlich isotherm was also applied to estimate the adsorption intensity of the adsorbate on the adsorbent surface. From the examination of the plot of  $\log q_e$  versus  $\log C_e$ ,

**Table 2.** The adsorption isotherms models and their parameters.

Isotherm	Constants	MB	MO
Langmuir	$q_m a_X$ (mg/g)	9.637	7.183
	$K_L$ (Lmg <sup>-1</sup> )	0.3603	0.2255
	$R^2$	0.9492	0.9223
Freundlich	$K_F$	3.497	3.545
	$N$	4.902	6.569
	$R^2$	0.9932	0.9943
Dubinin Radush-Kevich	$\beta$ (mol <sup>2</sup> /KJ <sup>2</sup> )	1.667x10 <sup>-8</sup>	1.779x10 <sup>-8</sup>
	$E$ (KJ/mol)	1.733	0.5301
	$q_0$ (mg/g)	2.143	1.476
	$R^2$	0.9199	0.8564
Temkin	$A$ (L/g)	105.9	53.58
	$b$ (kJ/mol)	3.355	4.368
	$R^2$	0.8457	0.8093
Scatchard	$q_m$	6.799	5.0979
	$b$	1.797	1.2817
	$R^2$	0.5392	0.4596

the  $R^2$  values of 0.99321 and 0.994426 (Figure 6) reveal that Freundlich isotherm fits better than the Langmuir model. This suggests that the adsorption of both dyes occur on heterogeneous binding sites with different binding energies. The constant,  $1/n$ , is a measure of the surface heterogeneity, when it is less than 1. The closer it is to zero, the more heterogeneous it is. Also, the adsorption is favorable when  $n$  has value between 0 and 10. In this case, the adsorption of both dyes onto Rf is favourable as  $n$  is 4.902 and 6.569 for MB and MO respectively (Table 2). The inverse of these values indicate surface heterogeneity.

Furthermore, the Scatchard plot (Figures 8a and b) provided further confirmation of the heterogeneity of the binding sites in that a linear outcome indicates the presence of only one kind of binding site (homogeneity) and vice-versa. The  $R^2$  values of 0.53915 for MB and 0.45962 for MO (Figures 8a and b) clearly shows a deviation from linearity meaning that the Rf surface is heterogeneous and further supports the conclusion that the Freundlich model most suitably describes the mechanism. Again, the  $R^2$  values obtained for the D-R (Figures 7a and b) and the Temkin isotherms (Figures 8a and b) for both dyes indicated a poor fit to the experimental data. However the

D-R and Temkin parameters were estimated as described earlier and the corresponding parameters are also presented in Table 2.

### Adsorption kinetics

The results of the kinetic studies of the adsorption of MB and MO onto *Raphia farinifera* are summarized in Figure 10. Of the tested kinetic models, only the pseudo-second-order and Elovich kinetic models suitably fitted the experimental data for both dyes adsorption onto Rf. The linear relationship between  $t/qt$  and  $t$  with  $R^2$  close to unity (Figure 10b) is an indication that the second-order mechanism applies in the adsorption processes and suggests a chemical adsorption mechanism. The Elovich kinetic model also properly fits the kinetic data for both dyes adsorption processes (Figure 10d). This is further interpreted to mean that the process occurs by a chemisorption mechanism with the rate-determining step being the uptake of the dye molecules onto the active sites of the *Raphia farinifera* biomass. The intra-particle diffusion model also showed slight fitness only for the MO adsorption onto the Rf biomass with a correlation coefficient of 0.926641.

The meaning of this is that for the MO adsorption, intra-particle diffusion of the molecules onto the Rf surface occurs quite significantly but not as the rate-determining step,

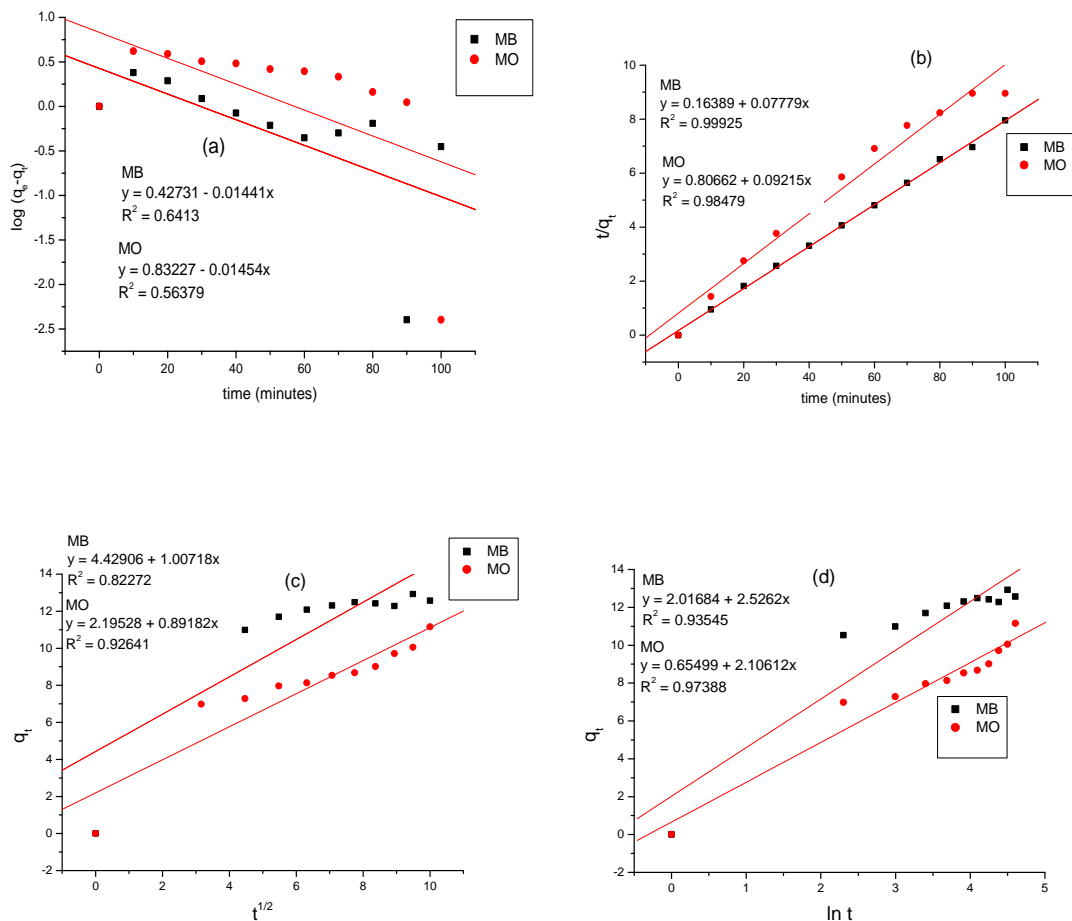


**Figure 10.** (a) pseudo first-order (b) Pseudo second-order (c) intra particle diffusion and (d) Elovich kinetic models for the adsorption of MB and MO dyes onto *Raphia farinifera* biomass.

because the linear plot of  $q_t$  vs  $t_{1/2}$  is not from the origin. If it had been from the origin, then the intra-particle diffusion model would be the rate-determining step for the process (Akpomie and Dawodu, 2015); however, there is an intercept (Figure 10c). The intercept represents the boundary layer effect and the greater the intercept, is, the more likely it is that surface sorption is the rate-determining step and the less the intercept, the less the contribution of capillary adsorption in the pores (Akpomie and Dawodu, 2015).

**CONCLUSION**

MB and MO dyes may be removed from aqueous systems by adsorption onto *Raphia farinifera* as the latter has been shown to have good affinity for the dyes. The process is kinetically feasible, simple and cheap. *Raphia farinifera* is therefore recommended as a cheap

alternative to activated carbon.

**ACKNOWLEDGEMENT**

The author is grateful to Mr Richard and his team for their help in the collection of the *Raphia farinifera* fruit bunches.

**CONFLICT OF INTERESTS**

The author has not declared any conflict of interests.

**REFERENCES**

**Akpomie Kovo G., Dawodu Folasegun A. and Adebowale Kayode O. (2015).** Mechanism on the sorption of heavy metals from binary-solution by a low cost montmorillonite and its desorption potential. *Alexandria Engineering Journal*, 54: 757 - 767

- Aksu, Z. (2005).** Application of biosorption for the removal of organic pollutants: A review. *Process Biochemistry*, 40 (3-4): 997–1026.
- Anirudhan, T.S. and Suchithra P.S. (2010).** Equilibrium, kinetic and thermodynamic modeling for the adsorption of heavy metals onto chemically modified hydrotalcite, *Industrial Journal of Chemical Technology*, 17: 247–259.
- Attia, A. A., Girgis, B. S. and Fathy, N. A. (2008).** Removal of methylene blue by carbons derived from peach stones by H<sub>3</sub>PO<sub>4</sub> activation: batch and column studies. *Dyes Pigments*, 76(1):282–289.
- Demirbas, E., Kobya, M. and Sulak, M. (2008).** Adsorption kinetics of a basic dye from aqueous solutions onto apricot stone activated carbon. *Bioresource Technology*, 99(13):5368–5373.
- Dubin, M. M. (1960).** The potential theory of adsorption of gases and vapors for adsorbents with energetically non uniform surfaces. *Chemical Reviews*, 60: 235-241.
- Freundlich, H. M. F. (1906).** Over the adsorption in solution. *Journal of Physical Chemistry*, 57: 385-471.
- Fytianos, K., Voudrias, E. and Kokkalis, E. (2000).** Sorption–desorption behavior of 2,4-dichlorophenol by marine sediments. *Chemosphere*, 40: 3–6
- Ghosh, D. and Bhattacharyya, K. G. (2002).** Adsorption of methylene blue on kaolinite. *Applied Clay Science*, 20: 295-300.
- Gupta, V. (2009).** Application of low-cost adsorbents for dye removal: a review. *Journal of Environmental Management*, 90 (8) : 2313 – 2342.
- Gupta, V.K., Pathania, D., Agarwal, S., and Singh P. (2012).** Adsorptional photocatalytic degradation of methylene blue onto pectin-CuS nanocomposite under solar light. *Journal of Hazardous Materials*, 243: 179-186.
- Hamza, I. A.A. Martincigh, B. S. Ngila, J. C. and Nyamori, V. O. (2013).** Adsorption studies of aqueous Pb(II) onto a sugarcane bagasse/multi-walled carbon nanotube composite. *Physics and Chemistry of the Earth*, 66: 157–166.
- Han, R., Ding, D., Xu, Y., Zou, W., Wang, Y., Li, Y. and Zou, L. (2008).** Use of rice husk for the adsorption of Congo red from aqueous solution in column mode. *Bioresource Technology*, 99 (8): 2938–2946.
- Ho, Y. S. (2003).** Removal of copper ions from aqueous solution by tree fern, *Water Research*, 37: 2323-2330.
- Horsfall, M. Spiff, A. I. and Abia, A. (2004).** Studies on the influence of Mercaptoacetic acid (MAA) Modification of cassava *Manihot culenta* Cran Waste Biomass on the adsorption of Cu<sup>2+</sup> and Cd<sup>2+</sup> from aqueous solution, *Bulletin of Korean Chemical Society*, 25: 969-976.
- Inyinbor, A.A., Adekola, F. A. and Olatunji, G. A. (2016).** Kinetics, isotherms and thermodynamic modelling of liquid phase adsorption of Rhodamine B dye onto *Raphia hookeri* fruit epicarp, *Water Resources and Industry*, 15: 14-27
- Khodaie Maryam, Ghasemi Nahid, Moradi , and Rahimi Mohsen. (2013).** Removal of Methylene Blue from Wastewater by Adsorption onto ZnCl<sub>2</sub> Activated Corn Husk Carbon Equilibrium Studies, *Journal of Chemistry*, 2013: 1-7.
- Kyzas, G. Z., Lazaridis, N. K. and Mi, A. C. (2012).** Removal of dyes from aqueous solutions with untreated coffee residues as potential low-cost adsorbents: equilibrium, reuse and thermodynamic approach. *Chemical Engineering Journal*. 189-190: 148–159.
- Lorenc-Grabowska, E. and Gryglewicz, G. (2007).** Adsorption characteristics of Congo red on coal-based mesoporous activated carbon. *Dyes Pigments*. 74(1): 34–40.
- Metivier-Pignon, H., C. Faur-Brasquet and P.L. Cloirec, (2003).** Adsorption of dyes onto activated carbon cloths: Approach of adsorption mechanisms and coupling of ACC with ultrafiltration to treat coloured wastewaters. *Separation and Purification Technology*, 31: 3-11.

- Mustapha, M.U. and Halimoon, N. (2015).** Micro-organism and Biosorption of heavy metals in the environment, *Journal of microbial and biochemical technology*. Doi:10.4172/1948-5948.1000219.
- Overah, L. (2011).** Biosorption of Cr (III) from aqueous solution by the leaf biomass of *Calotropis procera* – ‘Bom bom.’ *Journal of Applied Science and Environmental Management*, 15: 87-95.
- Overah L.C, Iwegbue C.M.A., Babalola J.O., and Martincigh B.S. (2019).** Fabrication and characterisation of a Fe<sub>3</sub>O<sub>4</sub>/*Raphia farinifera* nanocomposite for application in heavy metal adsorption. *Environmental Technology and Innovation* 13: 11- 29.
- Perez, N. Sánchez, M. Rincón, G. and Delgado, L. (2007).** Study of the behaviour of metal adsorption in acid solutions on lignin using a comparison of different adsorption isotherms. *Latin American Applied Research*, 37: 157-162.
- Salleh, M.A.M., Mahmoud, D.K., Karim, W.A.W.A. and dris A. (2011).** Cationic and anionic dye adsorption by agricultural solid wastes: a comprehensive review, *Desalination*, 280 (1-3): 1-13.
- Sud, D., Mahajan, G., and Kau M.P. (2008).** Agricultural waste material as potential adsorbent for sequestering heavy metal ions from aqueous solutions – a review *Bioresource Technology*, 99: 6017-6027.
- Wang Jing, Xu Junqing and Wu Ning (2017).** Kinetics and equilibrium studies of methylene blue adsorption on 2D nanolamellar Fe<sub>3</sub>O<sub>4</sub>. *Journal of Experimental Nanoscience*, 12(1): 297-307.
- Weber, WJ. and Morris, J C. (1963).** Kinetics of adsorption on carbon from solution. *Journal of the Sanitary Engineering Division*, 89(31): 312.
- Yu, B. Zhang, Y. Shukla, A. Shukla, S. S. and Dorris, K. L. (2001).** The removal of heavy metals from aqueous solutions by sawdust adsorption-removal of lead and comparison of its adsorption with copper. *Journal of Hazardous Matetrials*, 84: 83-94.
- Zohre Shahryari, Ataallah Soltani Goharrizi and Mehdi Azadi (2010).** Experimental study of methylene blue adsorption from aqueous solutions onto carbon nano tubes. *International Journal of Water Resources and Environmental Engineering*, 2(2): 016-028.